ARL-TR-9007 ● AUG 2020

DEVCOM ARMY RESEARCH LABORATORY

Electrophoretic Deposition of Aluminum Nanoparticles through a Nanopatterned Resist

by Benjamin Cerjan, David Renard, Stephan Link, Naomi Halas, and Mark H Griep

Approved for public release; distribution is unlimited.

NOTICES

Disclaimers

The findings in this report are not to be construed as an official Department of the Army position unless so designated by other authorized documents.

Citation of manufacturer's or trade names does not constitute an official endorsement or approval of the use thereof.

Destroy this report when it is no longer needed. Do not return it to the originator.

ARL-TR-9007 ● AUG 2020

Electrophoretic Deposition of Aluminum Nanoparticles through a Nanopatterned Resist

Benjamin Cerjan, David Renard, Stephan Link, and Naomi J Halas
Rice University

Mark H Griep
Weapons and Materials Research Directorate, CCDC Army Research Laboratory

Approved for public release; distribution is unlimited.

REPORT DOCUMENTATION PAGE		Form Approved OMB No. 0704-0188

Public reporting burden for this collection of information is estimated to average 1 hour per response, including the time for reviewing instructions, searching existing data sources, gathering and maintaining the data needed, and completing and reviewing the collection information. Send comments regarding this burden estimate or any other aspect of this collection of information, including suggestions for reducing the burden, to Department of Defense, Washington Headquarters Services, Directorate for Information Operations and Reports (0704-0188), 1215 Jefferson Davis Highway, Suite 1204, Arlington, VA 22202-4302. Respondents should be aware that notwithstanding any other provision of law, no person shall be subject to any penalty for failing to comply with a collection of information if it does not display a currently valid OMB control number.
PLEASE DO NOT RETURN YOUR FORM TO THE ABOVE ADDRESS.

1. REPORT DATE *(DD-MM-YYYY)*	2. REPORT TYPE	3. DATES COVERED (From - To)
August 2020	Technical Report	January 2019–October 2019

4. TITLE AND SUBTITLE	5a. CONTRACT NUMBER
Electrophoretic Deposition of Aluminum Nanoparticles through a Nanopatterned Resist	W911NF1920056
	5b. GRANT NUMBER
	5c. PROGRAM ELEMENT NUMBER

6. AUTHOR(S)	5d. PROJECT NUMBER
Benjamin Cerjan, David Renard, Stephan Link, Naomi Halas, and Mark H Griep	5e. TASK NUMBER
	5f. WORK UNIT NUMBER

7. PERFORMING ORGANIZATION NAME(S) AND ADDRESS(ES)	8. PERFORMING ORGANIZATION REPORT NUMBER
Rice University Houston, TX 77025	

9. SPONSORING/MONITORING AGENCY NAME(S) AND ADDRESS(ES)	10. SPONSOR/MONITOR'S ACRONYM(S)
CCDC Army Research Laboratory ATTN: FCDD-RLW-MG Aberdeen Proving Ground, MD 21005-5066	11. SPONSOR/MONITOR'S REPORT NUMBER(S) ARL-TR-9007

12. DISTRIBUTION/AVAILABILITY STATEMENT

Approved for public release; distribution is unlimited.

13. SUPPLEMENTARY NOTES

ORCID ID(s): Benjamin Cerjan, 0000-0002-0166-295X; David Renard, 0000-0002-1917-679X; Stephan Link, 0000-0002-4781-930X; Naomi J Halas, 0000-0002-8461-8494; Mark H Griep, 0000-0001-6460-8304

14. ABSTRACT

Large-area plasmonic metasurfaces have attracted interest as potential tools for a wide range of applications, from color-changing “glass” to improved efficiency of solar cells. These potential applications necessitate the capability to fabricate such surfaces at scale. One potential approach to resolve this issue is to use chemically synthesized nanoparticles as the metallic elements in such a metasurface rather than traditional metallization steps such as sputtering or evaporation. This study focuses on efficient methods for driving the particles into an array and subsequent postprocessing steps to remove excess particles. Using electrophoretic deposition (EPD), nanoparticles modified to have a strong surface charge can be driven into a masking pattern on top of a conductor when a voltage is applied. Following deposition, a method for removing excess particles using a low-adhesion tape is demonstrated. While this EPD approach is not yet effective enough for scaling, it serves as a useful guide for how such depositions might be approached in the future.

15. SUBJECT TERMS

electrophoresis, aluminum, nanoparticles, plasmonic metasurface, electrophoretic deposition, EPD

16. SECURITY CLASSIFICATION OF:			17. LIMITATION OF ABSTRACT	18. NUMBER OF PAGES	19a. NAME OF RESPONSIBLE PERSON
a. REPORT	b. ABSTRACT	c. THIS PAGE			Mark Griep
Unclassified	Unclassified	Unclassified	UU	18	19b. TELEPHONE NUMBER (Include area code) (410) 306-4953

Standard Form 298 (Rev. 8/98)
Prescribed by ANSI Std. Z39.18

Contents

List of Figures

1. Introduction

Large-area nanophotonic and plasmonic metasurfaces have been steadily gaining attention as improved designs and fabrication methods have been developed. In particular, researchers have demonstrated laser-printing metasurfaces[1,2] and flexible metasurfaces[3–5] as well as a host of metasurfaces replicating traditional optical elements.[6–10] However, most of these approaches are inherently difficult to scale above a few square inches while those that can require expensive systems with integrated vacuum chambers or subsequent postprocessing metallization.[11–13] Alternative approaches to metallization are necessary to address this issue. Electrophoretic deposition (EPD) is a promising candidate to address this need as it uses chemically synthesized particles that can be grown in large volumes and only requires seconds to minutes to uniformly fill a patterned area.[14–17] This process works by using an applied electric field to drive charged nanoparticles toward a conducting surface. This method could be easily integrated into a roll-to-roll (R2R) process to facilitate large-area device fabrication. To ensure this process is affordable at scale, as traditional plasmonic materials such as gold (Au) and silver are prohibitively expensive, we focus here on aluminum (Al) as our plasmonic metal.

Al has attracted growing interest as a plasmonic material due to its low cost,[18] chemical stability due to a passivating layer of aluminum oxide,[19] and support for optical resonances over a wide band of frequencies.[20–24] However, it remains challenging to fabricate large-area (>m^2) Al arrays or metasurfaces due to the necessity for pristine deposition of the Al to prevent oxidation throughout the structure, rather than only on the surface.[18] Using colloidally grown nanoparticles has advantages both in scalability and in the quality of the grown Al, as previous work has demonstrated the capability to grow single-crystalline particles.[25,26]

The aim of the present work is to adapt the EPD process for use with Al nanoparticles to enable the rapid and large-area deposition of plasmonic metasurfaces without the need for an evaporation chamber or other metallization technology. Initially, we reproduced previous[16] experimental results using Au nanoparticles to verify the procedure and experimental details. Then, Al nanoparticles were synthesized, coated in polydopamine (PDA) followed by polydiallyldimethylammonium chloride (P-DADMAC) to modify their surface charge, and finally were deposited through resist masks by an applied static electric field. It proved necessary to doubly coat the particles in polymers to ensure they had sufficient surface charge to allow the electrophoretic process to function. This work demonstrates an approach that will allow future research to have a scalable

method for preparing Al nanoparticles for EPD and potential integration into a R2R process flow.

2. Experimental Procedure

2.1 Au Nanoparticle Preparation

Citrate-capped Au nanoparticles were purchased from Nanocomposix (AUCN50-1000M) and were diluted to a concentration of 30 μg/mL in deionized water. Then, 10% (by weight) of P-DADMAC (Sigma-Aldrich; molecular weight 400,000–500,000) was added to the solution, followed by sonication for 1 min to uniformly coat the particles with the polymer. The solution was then washed three times in deionized water to remove excess polymer. Sodium chloride (NaCl) at various molarities was then added to the deionized water solution to make it sufficiently conductive for the EPD process. The particles were now stable for at least several months and ready for the EPD process.

2.2 Al Nanoparticle Preparation

The Al nanocrystals were grown and coated with PDA following previously described methods.[25,27] Following these processes, the PDA-coated Al nanoparticles were centrifuged out of their isopropanol (IPA) solution (at 12000 g) and resuspended in methanol (MeOH). Then, 10% (by weight) of P-DADMAC was added to the nanoparticle solution followed by ultrasonication for 1 min to uniformly coat the particles in the polymer. Next, the solution was washed three times in MeOH to remove excess polymer from the solution. At this point, the particles were stable in MeOH for several months and could be used for deposition as needed. Typical concentrations of Al nanoparticles in this solution were in the range of approximately 300 μg/mL.

2.3 Nanopattern Lithography

The masks for the deposition were made using standard clean-room fabrication methods. First, an indium tin oxide (ITO) slide (10 Ω-cm) was cleaned by sonicating in acetone for 3 min, followed by a 3-min plasma clean in argon (0.85 Torr, 200 W). Then, 400 nm of Microchem polymethyl methacrylate (PMMA) A4 was spun onto the substrate. Patterns were written into the PMMA using an FEI Quanta 650 scanning electron microscope (SEM) operating at 30 kV with a beam current of 30 pA for a total dose of 350 μC/cm^2. The substrates were then developed in a 1:3 mixture of methyl isobutyl ketone (MIBK):IPA for 50 s before being rinsed with IPA and blown dry with nitrogen.

2.4 EPD

For both Au and Al depositions, the patterned substrate was attached to an SEM stub to ensure electrical contact between the voltage source and the ITO-coated side of the substrate. The substrate was then inverted into the nanoparticle solution (approximately 60 µL) and a field of 0.6 V/mm was applied for 10 s (Fig. 1). Following deposition, the substrate was rinsed with IPA to clean off any residual MeOH or particles that were not well-adhered to the surface. Finally, low-adhesion tape (3M no. 3051) was optionally used to remove large clusters of nanoparticles not residing within one of the patterned locations.

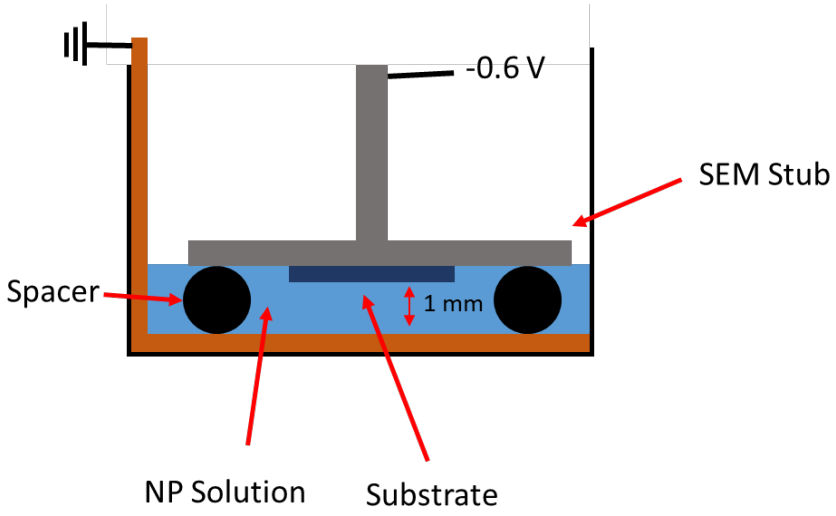

Fig. 1 Schematic diagram of EPD holder and process showing spacer, nanoparticle (NP) solution, patterned substrate, SEM stub, and electrical connections

Deposition of gold particles was achieved using approximately 60 µL of the as-prepared solution with no further modifications.

For depositions of Al particles, an aliquot of the prepared P-DADMAC coated particles in MeOH was diluted in deionized water with 6 mM of NaCl added, to achieve a nanoparticle concentration of approximately 50 µg/mL before being pipetted into the EPD holder. Note that the particles are only stable in water for a day or two before they fully oxidize, so this step should be done immediately prior to their deposition.

2.5 Characterization

A Malvern Zetasizer Nano ZS was used to determine the ζ-potential of the particles coated with PDA as well as particles coated with both PDA and P-DADMAC. Transmission electron microscopy (TEM) was used to verify the quality of the

surface coatings applied to the Al nanoparticles. SEM was used to determine nanoparticle filling fraction of the templated and deposited samples.

3. Results

To verify our experimental procedure, Au nanoparticles in solutions with different concentrations of NaCl were deposited through our templates as seen in Fig. 2a and b. It was found experimentally that the conditions for achieving high-quality depositions are constrained by surprisingly small tolerances. For too-low or too-high solution conductivity, as controlled by NaCl concentration, no substantial deposition occurs. It was found for our deposition conditions that a concentration of 6-mM NaCl in solution was optimal. Under this condition, EPD of Au particles produces very high filling fractions with almost no particles deposited on the surface of the template (see Fig. 2b).

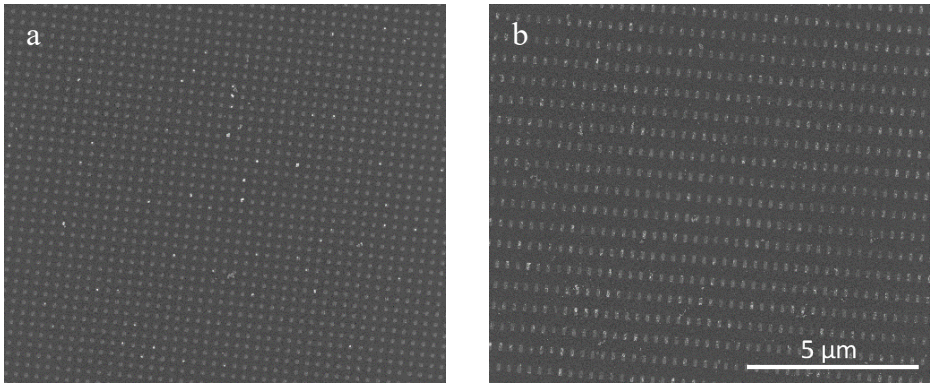

Fig. 2 EPD of Au nanoparticles in solution with differing concentrations of NaCl: a) 5-mM NaCl into 100-nm squares and b) 6-mM NaCl into 100- × 400-nm rectangles; as salt concentration increases, substantial improvement occurs in quality and filling fraction of deposition

Following the successful deposition with Au particles, a similar process was undertaken with Al nanoparticles. Al nanoparticles at various stages of coating are shown in Fig. 3a–c. The modifications to the surface of the Al particles do not deteriorate the particles and allow the nanocrystals to maintain their shape, not rounding the corners or extending more than a few nm beyond the edge of the particle. The layer of P-DADMAC is too thin to be distinguished from the PDA layer.

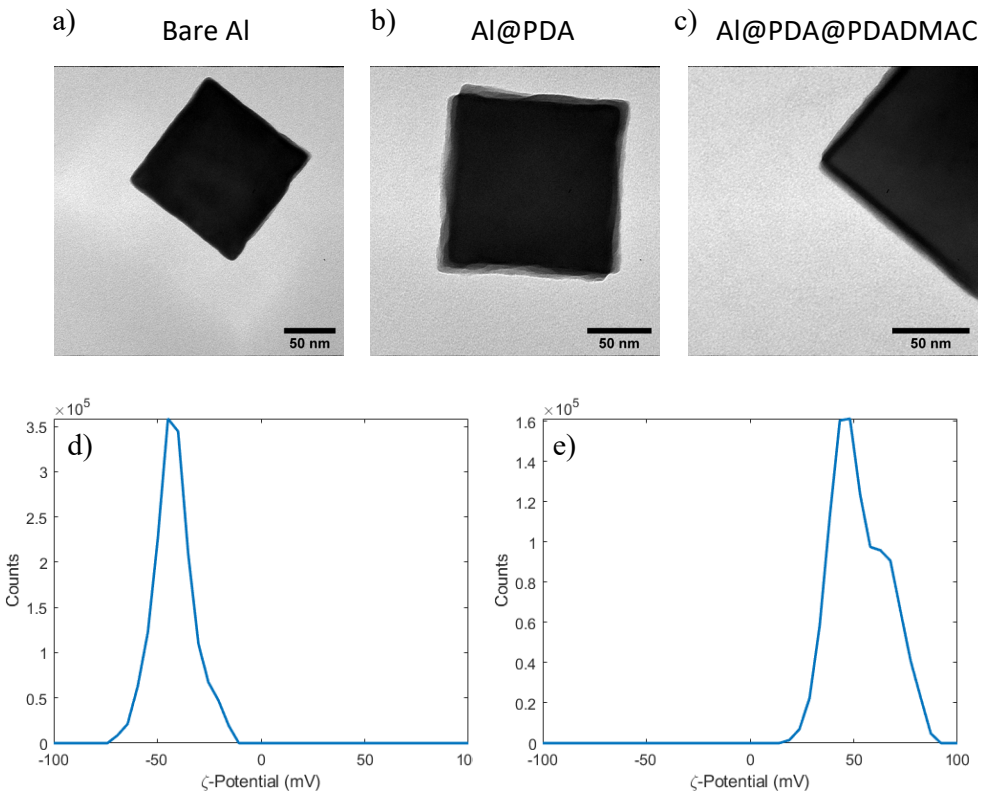

Fig. 3 a), b), and c) TEM images and d) and e) ζ-potential of Al nanocrystals in their PDA-coated and PDA- and P-DADMAC-coated states, respectively

The addition of the PDA and P-DADMAC layers clearly influence the ζ-potential as measured in MeOH, as seen in Fig. 3d and e. Following the synthesis and initial coating with the PDA layer the particles are negatively charged (–40 mV), and the P-DADMAC layer causes them to become strongly positively charged (+50 mV). This increase in surface charge is of importance as it helps to promote colloidal stability of the nanoparticles when they are added to the water for the deposition process and aids in preventing flocculation while suspended in the MeOH. Without the addition of the P-DADMAC, it was found the particles tended to clump together and deposit as large clusters instead of individual nanoparticles. As the EPD process requires a sufficiently conductive solution, the particles cannot be directly deposited out of the MeOH solution where they are stable and must first be transferred into a solution of deionized water and NaCl.

Results following a deposition can be seen in Fig. 4. Typical filling fractions were on the order of 15% for particles deposited into 1-μm-diameter holes in the resist mask. The method produces individual particle-binding events as can be seen in some of the wells, but there is still an unsatisfactory level of aggregation and nonspecific binding. In addition, the filling fraction is quite low, and we were unable to increase it by adjusting any of the experimental parameters at our

disposal. Increasing the deposition time increased nonspecific binding events, increasing the nanoparticle concentration produced yet larger clusters, and increasing the deposition field strength started to destroy the conductive ITO layer on the substrate.

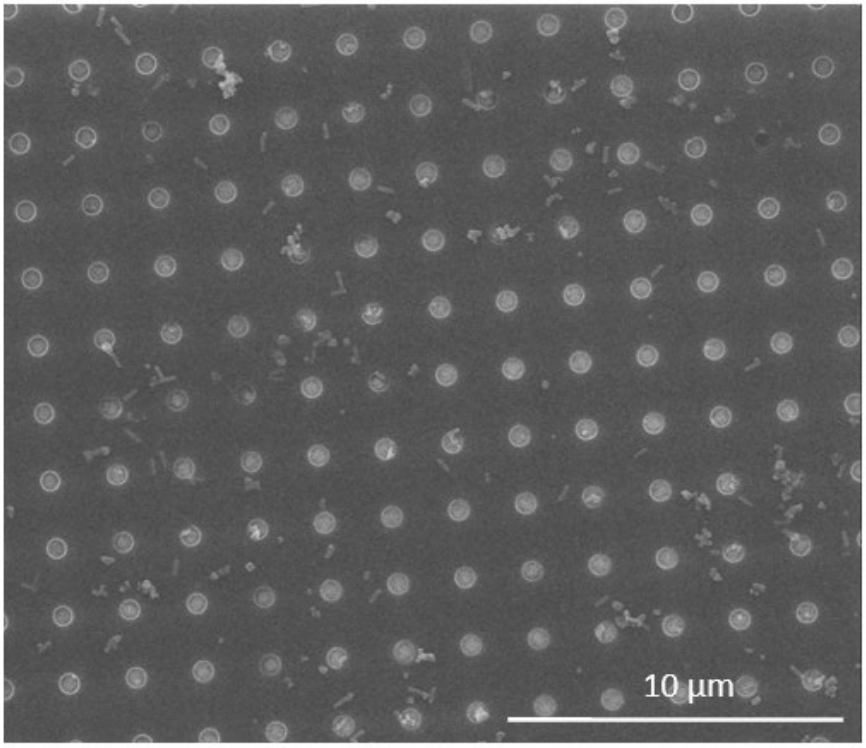

Fig. 4 Electrophoretically deposited Al nanoparticles through a PMMA template; holes are 1-µm diameter

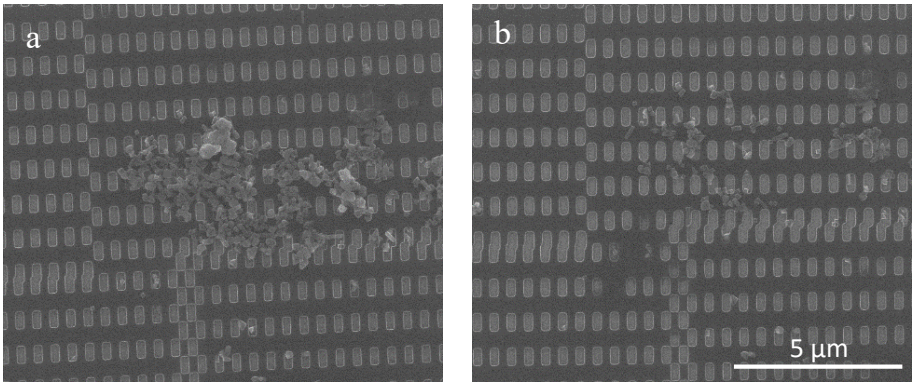

Fig. 5 SEM image of Al nanoparticle clusters on surface of a pattern a) before and b) after, using low-adhesion tape to remove excess particles

In addition to depositing particles, the ability to remove excess particles stuck to the surface of the template was investigated. Low-adhesion tape was used to gently remove particles and clusters not settled into a predefined well. As can be seen from

Fig.5, this is quite effective at removing particles in large clusters on the surface while leaving particles in the array in place. This method would be a suitable postprocessing step enabling a R2R process to efficiently remove excess particles.

4. Conclusion

In this work, Al nanocrystals had their surface chemistry modified, were deposited using EPD through a template, and were then selectively removed using low-adhesion tape. TEM images of the particles indicate the surface modifications do not adversely affect them. The surface modification of the nanoparticles is necessary to facilitate the EPD process, which under the studied conditions only reaches a 15% filling fraction of the template. Removing excess particles using low-adhesion tape was found to be quite effective and should allow for leniency in how specifically particles can be directed exclusively into the template. Although this work is only able to achieve a fairly low filling fraction, it clearly demonstrates that Al particles can also undergo the EPD process successfully and with further chemical modifications might be able to reach complete filling of the template. This work gives some guidance as to how metasurfaces could be rapidly produced as all the techniques used here, except the initial lithography, which could be replaced with nanoimprinting, are readily applicable to R2R scale up.

5. References

1. Zhu X, Vannahme C, Højlund-Nielsen E, Mortensen NA, Kristensen A. Plasmonic colour laser printing. Nat Nanotechnol. 2016;11(4):325–329. https://doi.org/10.1038/nnano.2015.285.

2. Zhu X, Yan W, Levy U, Mortensen NA, Kristensen A. Resonant laser printing of structural colors on high-index dielectric metasurfaces. Sci Adv. 2017;3(5):1–9. https://doi.org/10.1126/sciadv.1602487.

3. Li PC, Yu ET. Flexible, low-loss, large-area, wide-angle, wavelength-selective plasmonic multilayer metasurface. J Appl Phys. 2013;114(13). https://doi.org/10.1063/1.4824371.

4. Yoo D, Johnson TW, Cherukulappurath S, Norris DJ, Oh SH. Template-stripped tunable plasmonic devices on stretchable and rollable substrates. ACS Nano. 2015;9(11):10647–10654. https://doi.org/10.1021/acsnano.5b05279.

5. Liu X, Wang J, Tang L, Xie L, Ying Y. Flexible plasmonic metasurfaces with user-designed patterns for molecular sensing and cryptography. Adv Funct Mater. 2016;26(30). https://doi.org/10.1002/adfm.201601154.

6. Chen S, Reineke B, Li G, Zentgraf T, Zhang S. Strong nonlinear optical activity induced by lattice surface modes on plasmonic metasurface. Nano Lett. 2019;19(9):6278–6283. https://doi.org/10.1021/acs.nanolett.9b02417.

7. Lu DY, Cao X, Wang KJ, He MD, Wang D, Li J, Zhang XM, Liu L, Luo JH, Li Z, et al. Broadband reflective lens in visible band based on aluminum plasmonic metasurface. Opt Express. 2018;26(26):34956–34964. https://doi.org/10.1364/oe.26.034956.

8. Wang W, Guo Z, Li R, Zhang J, Liu Y, Wang X, Qu S. Ultra-thin, planar, broadband, dual-polarity plasmonic metalens. Photonics Res. 2015;3(3):68–71. https://doi.org/10.1364/prj.3.000068.

9. Xu Q, Zhang X, Xu Y, Li Q, Li Y, Ouyang C, Tian Z, Gu J, Zhang W, Zhang X, et al. Plasmonic metalens based on coupled resonators for focusing of surface plasmons. Sci Rep. 2016;29(6):37861. https://doi.org/10.1038/srep37861.

10. Jin C, Zhang J, Guo C. Metasurface integrated with double-helix point spread function and metalens for three-dimensional imaging. Nanophotonics. 2019;8(3). https://doi.org/10.1515/nanoph-2018-0216.

11. Højlund-Nielsen E, Clausen J, Mäkela T, Thamdrup LH, Zalkovskij M, Nielsen T, Li Pira N, Ahopelto J, Mortensen NA, Kristensen A. Plasmonic colors: toward mass production of metasurfaces. Adv Mater Technol. 2016;1(7):1–8. https://doi.org/10.1002/admt.201600054.

12. Murthy S, Pranov H, Feidenhans'l NA, Madsen JS, Hansen PE, Pedersen HC, Taboryski R. Plasmonic color metasurfaces fabricated by a high speed roll-to-roll method. Nanoscale. 2017;9(37):14280–14287. https://doi.org/10.1039/c7nr05498j.

13. James TD, Mulvaney P, Roberts A. The plasmonic pixel: large area, wide gamut color reproduction using aluminum nanostructures. Nano Lett. 2016;16(6):3817–3823. https://doi.org/10.1021/acs.nanolett.6b01250.

14. Giersig M, Mulvaney P. Preparation of ordered colloid monolayers by electrophoretic deposition. Langmuir. 1993;9(12):3408–3413. https://doi.org/10.1021/la00036a014.

15. Islam MA, Herman IP. Electrodeposition of patterned CdSe nanocrystal films using thermally charged nanocrystals. Appl Phys Lett. 2002;80(20):3823–3825. https://doi.org/10.1063/1.1480878.

16. Zhang H, Cadusch J, Kinnear C, James T, Roberts A, Mulvaney P. Direct assembly of large area nanoparticle arrays. ACS Nano. 2018;12(8):7529–7537. https://doi.org/10.1021/acsnano.8b02932.

17. Xu Z, Jiang D, Wei Z, Chen J, Jing J. Fabrication of superhydrophobic nano-aluminum films on stainless steel meshes by electrophoretic deposition for oil-water separation. Appl Surf Sci. 2018;427:253–261. https://doi.org/10.1016/j.apsusc.2017.08.189.

18. Knight MW, King NS, Liu L, Everitt HO, Nordlander P, Halas NJ. Aluminum for plasmonics. ACS Nano. 2014;8(1):834–840. https://doi.org/10.1021/nn405495q.

19. Chen Y, Xin X, Zhang N, Xu YJ. Aluminum-based plasmonic photocatalysis. Part Part Sys Character. 2017;34. https://doi.org/10.1002/ppsc.201600357.

20. Sobhani A, Knight MW, Wang Y, Zheng B, King NS, Brown LV, Fang Z, Nordlander P, Halas NJ. Narrowband photodetection in the near-infrared with a plasmon-induced hot electron device. Nat Commun. 2013;4:1643. https://doi.org/10.1038/ncomms2642.

21. King NS, Liu L, Yang X, Cerjan B, Everitt HO, Nordlander P, Halas NJ. Fano resonant aluminum nanoclusters for plasmonic colorimetric sensing. ACS Nano. 2015;9(11):10628–10636. https://doi.org/10.1021/acsnano.5b04864.

22. Cerjan B, Halas NJ. Toward a nanophotonic nose: a compressive sensing-enhanced, optoelectronic mid-infrared spectrometer. ACS Photonics. 2019;6(1):79–86. https://doi.org/10.1021/acsphotonics.8b01503.

23. Knight MW, Liu L, Wang Y, Brown L, Mukherjee S, King NS, Everitt HO, Nordlander P, Halas NJ. Aluminum plasmonic nanoantennas. Nano Lett. 2012;12(11):6000–6004. https://doi.org/10.1021/nl303517v.

24. Tittl A, Michel AK U, Schäferling M, Yin X, Gholipour B, Cui L, Wuttig M, Taubner T, Neubrech F, Giessen H. A switchable mid-infrared plasmonic perfect absorber with multispectral thermal imaging capability. Adv Mater. 2015;27(31):4597–4603. https://doi.org/10.1002/adma.201502023.

25. McClain MJ, Schlather AE, Ringe E, King NS, Liu L, Manjavacas A, Knight MW, Kumar I, Whitmire KH, Everitt HO, et al. Aluminum nanocrystals. Nano Lett. 2015;15(4):2751–2755. https://doi.org/10.1021/acs.nanolett.5b00614.

26. Clark BD, Jacobson CR, Lou M, Renard D, Wu G, Bursi L, Ali AS, Swearer DF, Tsai AL, Nordlander P, et al. Aluminum nanocubes have sharp corners. ACS Nano. 2019;13(8):9682–9691. https://doi.org/10.1021/acsnano.9b05277.

27. Renard D, Tian S, Ahmadivand A, Desantis CJ, Clark BD, Nordlander P, Halas NJ. Polydopamine-stabilized aluminum nanocrystals: aqueous stability and benzo[a]pyrene detection. ACS Nano. 2019;13(3);3117–3124. https://doi.org/10.1021/acsnano.8b08445.

List of Symbols, Abbreviations, and Acronyms

Al	aluminum
Au	gold
EPD	electrophoretic deposition
IPA	isopropanol
ITO	indium tin oxide
MeOH	methanol
MIBK	methyl isobutyl ketone
NaCl	sodium chloride
PDA	polydopamine
P-DADMAC	polydiallyldimethylammonium chloride
PMMA	polymethyl methacrylate
R2R	roll-to-roll
SEM	scanning electron microscope
TEM	transmission electron microscope

1 (PDF)	DEFENSE TECHNICAL INFORMATION CTR DTIC OCA
1 (PDF)	CCDC ARL FCDD RLD CL TECH LIB
2 (PDF)	CCDC ARL FCDD RLW MG MH GRIEP JL LENHART